

Synthesis and Characterization of Hexagonal Mesoporous Aluminophosphates

P. Selvam* and S.K. Mohapatra

Solid State and Catalysis Laboratory, Department of Chemistry,
Indian Institute of Technology–Bombay, Powai, Mumbai 400076, India

(Received 7th October 2004)

Abstract

Thermally stable hexagonal mesoporous aluminophosphate molecular sieves were synthesized hydrothermally and characterized systematically using various analytical and spectroscopic techniques. Effects of various synthesis parameters, viz., pH, time, temperature, Al/P ratio, amount of surfactant, etc. were also studied.

INTRODUCTION

Since the discovery of microporous aluminophosphate (APO_n) molecular sieves in the early 1980s, these materials have been widely used in catalysis, separation, host–guest assemblies and as advanced functional materials.^{1,2} In the search of effective synthesis procedures that afford solids with larger pore channels, molecular sieves such as cloverite³ and VPI-5⁴ have been synthesized. Although, these systems have opened up new prospects in catalysis research, they limit their access to only small reactant molecules. On the other hand, the utilization of supramolecular arrays of organic amphiphiles as structure directing agents in the synthesis lead to the discovery of mesoporous materials of the type hexagonal MCM-41 with unidimensional pore system and cubic MCM-48 with three dimensional pore system.⁵ These materials combine the properties of microporous analogues, which are flexible enough to incorporate a wide variety of heteroatoms in their framework, and of extra-large pore systems, where the presence of mesopores allows the access of bulky organic molecules. However, the potential use of transition metal ion substituted MCM-41 / MCM-48 materials in the area of heterogeneous catalysis^{6,7} has triggered off considerable interest in the synthesis of their aluminophosphate analogues. Many of these materials have hexagonal and/or lamellar structures that are thermally unstable⁸⁻²⁰ while

some of the products do exhibit mesoporosity in a hexagonal or disordered arrangement.²¹⁻³⁷ This is mainly attributed to the narrow range of formation of thermally stable hexagonal mesoporous aluminophosphate (HMA) phase as compared to the unstable lamellar mesoporous aluminophosphate (LMA) phase, which has made the synthesis of this material extremely difficult. Therefore, it is important to optimize the synthesis conditions so that high quality single phase HMA can be prepared in a reproducible manner. Here, we report, on the synthesis and characterization of HMA molecular sieves and the various parameters affecting the formation of the phase.

EXPERIMENTAL

Starting Materials

Phosphoric acid (85 %, Qualigens); aluminium isopropoxide (97 %, Merck); tetramethyl ammonium hydroxide (TMAOH, 25 wt % in water, Aldrich); cetyltrimethylammonium chloride (CTAC, 25 wt % in water, Aldrich); Aluminium sulphate (98 %, Aldrich); Aluminium nitrate (99 %, Aldrich); Sodium hydroxide (98 %, Loba); Sodium aluminate (50-56 % Al; Fluka); potassium hydroxide (85 %, S.D. fine), ammonium hydroxide (25 %, S.D. fine chemicals). Aluminophosphate (AlPO₄; 99 %, Aldrich) was used as standard for the MAS-NMR measurements.

*Corresponding author. E-mail: selvam@iitb.ac.in

Table 1. Experimental conditions for the synthesis of mesoporous aluminophosphates.

Gel (molar) composition	Reaction condition	Fig.	Observation	Notation	Inference
1 Al ₂ O ₃ : 1 P ₂ O ₅ : 1 CTAC : 2.5 TMAOH : 60 H ₂ O	373 K, 3 d, pH = 10.0	1a	Well-crystallized or ordered HMA	WH	In addition to 100 main reflection, higher order reflections, viz., 110, 200 and 210 appear.
1 Al ₂ O ₃ : 1 P ₂ O ₅ : 1 CTAC : 2.5 TMAOH : 60 H ₂ O	373 K, 5 d, pH = 10.0	1b	Poorly-crystallized or disordered HMA	PH	Only 100 reflection is observed indicating disordered hexagonal (tubular) structure.
1 Al ₂ O ₃ : 1 P ₂ O ₅ : 1 CTAC : 2.5 TMAOH : 60 H ₂ O	403 K, 3 d, pH = 10.0	1c	Well-crystallized LMA	L	In addition to 100 reflection, the reflections of higher order viz., 110, 200 and 210 also appear.
1 Al ₂ O ₃ : 1 P ₂ O ₅ : 1 CTAC : 2.5 TMAOH : 60 H ₂ O	403 K, 1 d, pH = 10.0	1d	Mixed phases with more LMA and less HMA	L+H	Reflections corresponding to lamellar phase were more prominent than hexagonal phase.
1 Al ₂ O ₃ : 1 P ₂ O ₅ : 1 CTAC : 2.5 TMAOH : 60 H ₂ O	383 K, 5 d, pH = 10.0	1e	Mixed phase with more HMA and less LMA	H+L	Reflections corresponding to hexagonal phase were more prominent as compared to lamellar phase.
1 Al ₂ O ₃ : 1 P ₂ O ₅ : 1 CTAC : 2.5 TMAOH : 60 H ₂ O	423 K, 3 d, pH = 10.0	--	Unidentified microporous or dense phases	U	No reflection in lower 2θ region but some in higher 2θ region was observed.

Synthesis of HMA

The synthesis of thermally stable HMA was performed by the following procedure with a final molar gel composition was: Al₂O₃ : P₂O₅ : CTAC : 2.5 TMAOH : 60 H₂O. At first, phosphoric acid (1.4 ml) and water (11.7 ml) were mixed followed by a slow addition of aluminium isopropoxide (4.08 g) under vigorous stirring at 343 K until a clear solution was obtained. To this solution, TMAOH (7.3 ml) was added drop-wise followed by CTAC (13.22 ml). The mixture was further stirred for 12 h until a clear homogeneous gel was formed. It was then transferred into a Teflon-lined autoclave and heated in an air oven at 373 K for 72 h. The resultant solid products were repeatedly washed with distilled water, filtered, and dried at 343 K for 12 h. The as-synthesized HMA was then calcined at 823 K for an hour under flowing nitrogen followed by 2 h in air. In order to obtain the best conditions for the preparation of stable HMA, optimization of gel composition

with time, temperature and pH was performed. Various structures obtained by this way were analyzed by powder X-ray diffraction (XRD). Table 1 summarizes the various preparative conditions employed and the different structures obtained. The representative diffraction patterns are presented Fig. 1.

Characterization

The as-synthesized and calcined samples were characterized using several analytical and spectroscopic techniques. Powder X-ray diffraction (XRD) patterns were recorded on a Rigaku-miniflex diffractometer using a nickel filtered Cu-Kα radiation ($\lambda = 1.5418 \text{ \AA}$) and a step size of 0.02° . Transmission electron micrograph (TEM) image and electron diffraction (ED) were recorded on a Philips 200 microscope operated at 160 kV. The sample (in fine powdered form) was dispersed in ethanol with sonication (Oscar ultrasonics) and placed a drop of it on a carbon coated copper grid (300

mesh; Sigma-Aldrich). Thermogravimetry / differential thermal analysis (TGA/DTA) measurements were performed using ~ 15 mg of the sample on a Dupont 9900/2100 TGA/DTA system under nitrogen atmosphere (40 ml min⁻¹) with a heating rate of 10 K min⁻¹.

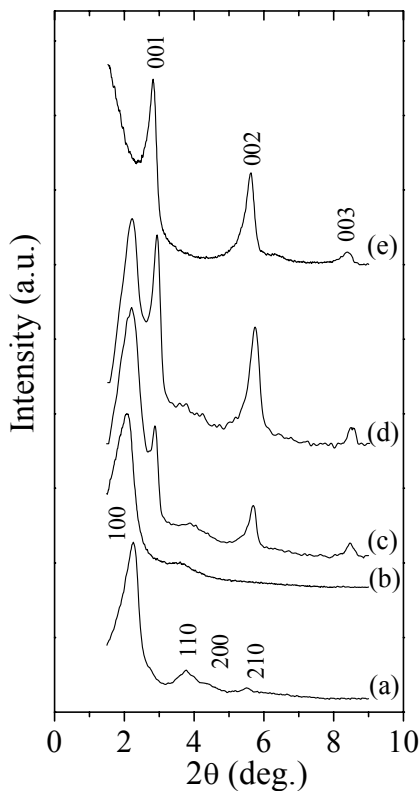


Figure 1. XRD patterns of: (a) WH, (b) PH, (c) H+L, (d) L+H and (e) L. See also Table 1.

Surface area analysis was performed on a Sorptomatic-1990 instrument. Before measurement, the calcined sample was evacuated at 523 K for 12 h under vacuum (10⁻³ torr). The surface area was calculated using the BET (Brunauer-Emmett-Teller) method and the pore size was calculated using the Horvath-Kawazoe method. The pore volume was determined from the amount of N₂ adsorbed at P/P₀ = 0.5. The elemental analysis of the various samples was carried out by inductively coupled plasma-atomic emission spectroscopy ICP-AES technique on Labtam Plasma Lab 8440 equipment. The acidic behavior of the catalyst was studied by temperature programmed desorption of ammonia (TPDA). About 400 mg of sample was placed in quartz reactor and was activated at 823 K in air for 6 h followed by 2 h in helium (with a flow rate of 50 ml min⁻¹). Then the reactor was cooled to 373 K

and maintained for another hour under the same condition. Ammonia adsorption was carried out by passing the gas through the sample for 15-20 min at this temperature. Subsequently, it was purged with helium for an hour to remove the physisorbed ammonia. The desorption of ammonia was carried out by heating the reactor up to 873 K at a rate of 10 K min⁻¹ using a temperature programmer (Eurotherm). The amount of ammonia desorbed was estimated with the aid of thermal conducting detector (TCD) response factor for ammonia.

RESULTS AND DISCUSSION

Effect of synthesis parameters on the formation of HMA

Table 1 presents the optimized experimental conditions for the preparation of mesoporous aluminophosphate molecular sieves. Figure 1 depicts the corresponding XRD patterns of different samples. It can be seen from this table and the figure that well crystallized HMA was obtained for the initial gel composition of: 1 Al₂O₃ : 1 P₂O₅ : 1 CTAC : 2.5 TMAOH : 60 H₂O with reaction condition of 373 K, 3 d and pH = 10.0. However, various synthesis parameters affect the formation of single-phase HMA. Therefore, it is considered that the control of the framework structure is the most important for the synthesis of thermally stable HMA and thermally unstable LMA.

Effect of pH: The pH of the final gel plays a crucial role in the formation of the different phases as it drives the solubility of all the ingredients and therefore produces a clear homogeneous gel. In addition to this, it also takes a major part in the initial arrangement of the surfactants to a particular array upon which the inorganic species condense to give the required polymerized material. In this investigation, the pH was varied from 7.6 to 11.0, and for this purpose, TMAOH was used. Thus, the final gel (molar) composition of the gel was: 1 Al₂O₃ : 1 P₂O₅ : 1 CTAC : x TMAOH : 60 H₂O (x = 0-3). Table 2 summarizes the salient results. It is noteworthy here that no mesostructured products were obtained under a pH ≤ 2.5 or TMAOH free condition (pH = 2.5). At lower pH, only well crystalline lamellar phase was obtained (Table 2). On increasing the pH, HMA

starts forming along with LMA, but at pH = 10, only a single-phase HMA results. At still higher pH (≤ 10.5), a disordered hexagonal phase was obtained, which has a low thermal stability as compared to well-crystallized HMA. On the other hand, when pH was increased >10.5 , only LMA was obtained. However, the reason for the formation of LMA both at higher and lower pH values is not clear.

Table 2. Effect of pH on the formation of HMA.^a

pH	x (mole)	Crystallization time (d)	Phase
7.6	1.1	3, 5	L; L
8.4	1.6	3, 5	L+H; L
9.2	2.0	3, 5	H+L; L
10.0	2.5	3, 5	WH; H
10.5	2.8	3, 5	H; L+H
11.0	3.0	3, 5	L; L

^a Gel (molar) composition: 1 Al₂O₃ : 1 P₂O₅ : 1 CTAC : x TMAOH : 60 H₂O, T = 373 K. For structure notation, see Table 1.

Effect of crystallization time and temperature:

Table 3 presents the results of the various phases formed under different crystallization temperature and duration of the reaction. In the specified gel composition and keeping a constant pH (= 10), we synthesized pure hexagonal phase (PH) with a broad XRD peak (stirring at RT for 48 h). Under hydrothermal conditions, the best phase (WH) was formed at 373 K and duration for 72 h (Table 3).

Table 3. Effect of time and temperature on the formation of HMA.^a

Crystallization temperature (K)	Crystallization time (d)	Phase
423	1, 3, 5	U
403	1, 3, 5	L+H; L; L
383	3, 5	H; H+L
373	3, 5	WH; H

^a Gel (molar) composition: 1 Al₂O₃ : 1 P₂O₅ : 1 CTAC : 2.5 TMAOH : 60 H₂O, pH = 10. For structure notation, see Table 1.

Increasing the time period under the same conditions decreased the order and crystallinity of the HMA phase. Increasing the temperature to 403 K resulted in formation of pure lamellar

phase. On increasing the temperature further gave rise to some unidentified phase (U). Hence, the optimized synthesis condition in the specified gel composition at pH 10 is 72 h at 373 K. On increasing the degree of condensation (i.e., increasing the time and temperature) leads to mixed, LMA or some unidentified phases. Thus, other studies discussed were performed hydrothermally at 373 K for 72 h.

Effect of Al/P (molar) ratio: The composition of the starting mixture was changed as follows: yAl₂O₃ : P₂O₅ : 1 CTAC : 2.5 TMAOH : 60 H₂O. To vary the Al/P molar ratio, we varied the number of moles of Al in the gel. Because the pH value changed with the variation in H₃PO₄, we kept the amount of H₃PO₄ constant. Thus, Al/P ratio was varied at constant pH = 10 by changing the number of moles aluminium isopropoxide. Table 4 lists the phases formed by changing the Al/P molar ratios in the starting gel. It indicates that HMA can be synthesized in a wide range of Al/P ratio of 0.75-1.25 (Table 4) at pH=10. At higher Al concentration, lamellar phase was found to form.

Table 4. Effect of Al/P molar ratio on the formation of HMA.^a

Y (mole)	Al / P (molar) ratio	Phase
0.5	0.50	H+L
0.75	0.75	WH
1.0	1.0	WH
1.25	1.25	H
1.5	1.5	H+L
2.0	2.0	L

^a Gel (molar) composition: yAl₂O₃ : P₂O₅ : 1 CTAC : 2.5 TMAOH : 60 H₂O; pH = 10, T = 373 K, t = 3 d. For structure notation, see Table 1.

Effect of surfactant concentration: In literature, cationic surfactants have been used to synthesize hexagonal phases of mesostructured aluminophosphates. Neutral or anionic surfactant gives rise to only lamellar phases. Only Lu et. al.³⁸ were able to synthesize cubic phase by varying the surfactant (cetyltrimethylammonium bromide) amount. Here, only LMA/HMA or mixed phases were obtained by varying the amount of surfactant. No intermediate cubic phase was observed. The

composition of the starting mixture was changed as follows: 1 Al₂O₃ : 1 P₂O₅ : z CTAC : x TMAOH : 60 H₂O. The change in pH by changing the amount of CTAC was compensated by TMAOH and in all the cases the final pH of the gel was kept around 10. It was observed that hexagonal phase can be obtained in the region z = 0.75 to 1 (Table 5). In all other cases, mixed or LMA phases were obtained. In the higher surfactant concentration only lamellar phase was obtained.

Table 5. Effect of surfactant concentration on the formation of HMA.^a

z (mole)	x (mole)	Phase
0.50	3.2	H+L
0.75	2.9	H
1.0	2.5	WH
1.25	2.3	L+H
1.50	2.0	L
2.0	1.8	L

^a Gel (molar) composition: 1Al₂O₃ : 1P₂O₅ : z CTAC : x TMAOH : 60H₂O, pH = 10, T = 373 K, t = 3 d. For structure notation, see Table 1.

Effect of water content: The composition of the starting mixture was changed as follows: 1 Al₂O₃ : 1 P₂O₅ : 1 CTAC : x TMAOH : u H₂O. A hexagonal mesostructured product was formed at u = 60-70 (Table 6). With the increase and decrease in the amount of water, LMA formed, instead of maintaining the pH at 10 by TMAOH.

Table 6. Effect of water on the formation of HMA.^a

u (mole)	x (mole)	Phase
40	2.2	H
60	2.5	WH
100	3.0	L+H
150	4.1	L
200	5.3	L

^a Gel (molar) composition: 1Al₂O₃ : 1P₂O₅ : 1CTAC : x TMAOH : u H₂O, pH=10, T = 373 K, t = 3 d. For structure notation, see Table 1.

Effect of different bases: The use of TMAOH as a base gave good quality materials. NaOH, KOH or NH₄OH resulted in the formation of only an amorphous material. The function of organic ammonium cation (TMA⁺) from TMAOH is

probably to modify the strength of the electrostatic interaction between the aluminophosphate species (Γ⁻) and the cationic surfactant micelle assembly (S⁺) to form the S⁺Γ⁻ / TMA⁺ ion pair. The details are discussed below in formation mechanism.

Effect of different aluminium sources: Different aluminum sources, viz., aluminum isopropoxide, aluminum nitrate, aluminium sulfate and sodium aluminate were employed for the preparation. The use of aluminium isopropoxide results in good quality HMA, while the use of aluminum sulfate gave hexagonal phase but of poor quality. On the other hand, aluminum nitrate did not give any solid product and that sodium aluminate produced amorphous material.

Single phase HMA

XRD/TEM/ED: Figure 2 shows the XRD patterns of good quality HMA. It can be seen from this figure that the as-synthesized HMA showed a typical diffraction pattern (Fig. 2a) with well defined reflections characteristic of hexagonal MCM-41 structure.^{5,7} The calculated average unit cell dimension (*a*₀) for as-synthesized HMA was 45.4 Å. On the other hand, the XRD patterns of calcined HMA (Figure 2b) showed a single broad reflection, i.e., 100, with *d*₁₀₀ = 39.4 Å and that the higher reflections, viz., 110, 200 and 210, disappeared. It is also clear from this figure that, upon calcination a decrease in unit cell dimension (*a*₀ = 33.7 Å) was observed due to the contraction of the framework as a consequence of the removal of the surfactant molecules. This may be due to finite size effects of very fine particle morphology or due to the more disordered hexagonal framework structure of the samples.⁴⁵ The results are ably supported by the TEM image and ED pattern of calcined HMA where the samples show disordered hexagonal pattern (Figure 3).⁴⁵⁻⁴⁷ Similar observations are noted for other systems such as HMS,⁴⁵ MSU-1,⁴⁶ KIT-1⁴⁷ in literature. On the other hand, XRD pattern of LMA consists of three main reflections (Fig. 4b; 001, 002 and 003) with *d*₀₀₁ = 31.5 Å. In addition to this, several other unidentified reflections were observed in higher 2θ regions, which could be attributed to excess surfactant present in the

structure. However, after calcination at 473 K for 3 h in air, the structure collapses and no reflections were observed (Fig. 4d) resulting in the formation of amorphous aluminophosphate phase. On the other hand, the HMA gives rise to disordered structure (Fig. 4c) with a small increase in amorphous aluminophosphate phase .

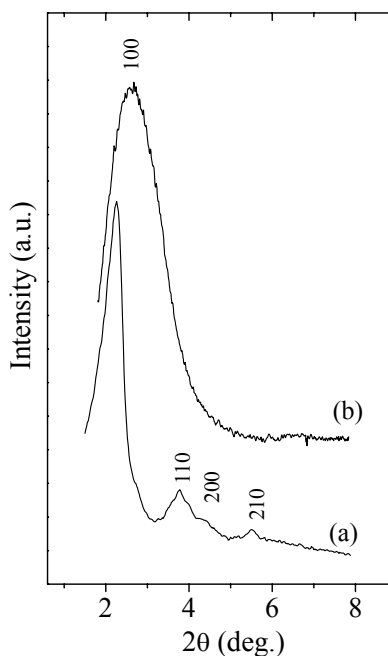


Figure 2. XRD patterns of: (a) as-synthesized HMA and (b) calcined HMA.

ICP-AES: ICP-AES analysis of calcined HMA samples showed Al/P ratio 1.31. It indicates that some of the Al species are involved independently in mesoporous material assembly without a neighbor P due to incomplete condensation. On the other hand, the Al/P molar ratio for LMA was found to be 1.13. This suggests the condensation in LMA is better than the HMA matrix. Thus, mesoporous aluminophosphate materials possesses a nonideal three-dimensional aluminophosphate framework different from microporous aluminophosphate molecular sieves, where Al/P = 1 is generally observed.⁴⁸

FT-IR: The FT-IR spectra of HMA and LMA also revealed significant differences between the two materials. Figure 5 shows the FT-IR spectra of as-synthesized HMA, LMA and calcined HMA. The sharp bands at 2827 and 2861 cm^{-1} correspond to the C-H stretching vibrations of the surfactants. The main difference in the two

materials was observed in the O-T-O asymmetric stretching region. HMA showed O-T-O asymmetric stretching at 1059 and 1126 cm^{-1} and LMA at 1038, 1164 and 1228 cm^{-1} .²⁵ The symmetric O-T-O stretching showed at 584 cm^{-1} for HMA and 575 cm^{-1} for LMA. After calcinations, the peaks corresponding to surfactant were not observed for HMA and the O-T-O asymmetric and symmetric stretching was observed at 1094 and 538 cm^{-1} , respectively.

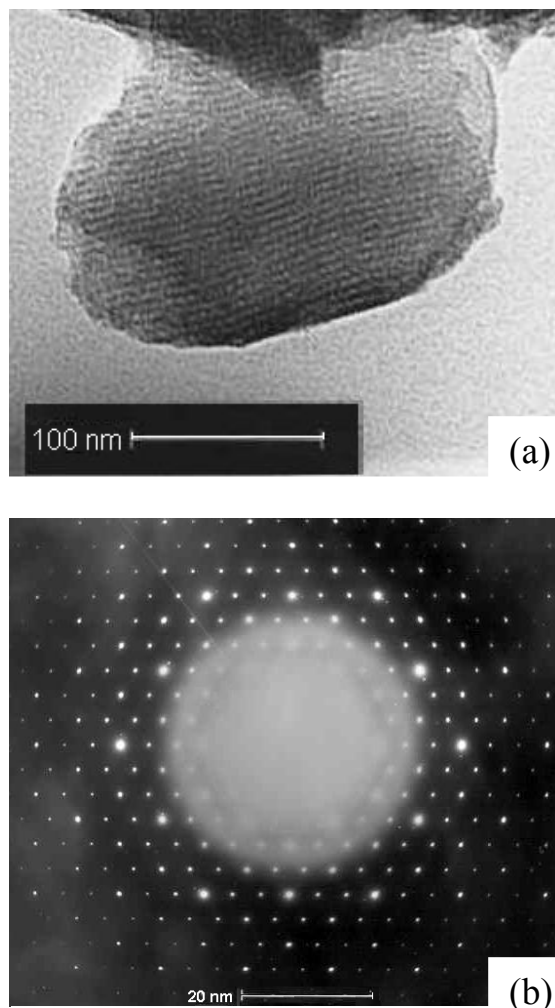


Figure 3. (a) TEM image and (b) ED of calcined HMA.

TG-DTA: Figure 6 shows TG-DTA of as-synthesized HMA, which gives a weight loss of 60 % on heating to 973 K. The total weight loss is attributed to the desorption of water or other atmospheric gaseous molecules, and decomposition of CTA and TMA ions.²⁶ TG-DTA of LMA showed the same type of thermogram. The calcined HMA (Figure 7) showed around 18 %, due to adsorbed water

and/or other gases, with a corresponding endotherm at 383 K in DTA.

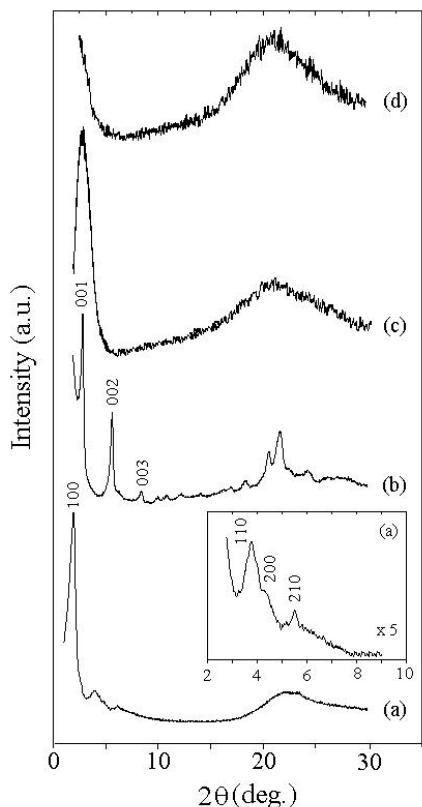


Figure 4. XRD patterns of: (a) as-synthesized HMA, (b) as-synthesized LMA, (c) calcined HMA and (d) calcined LMA.

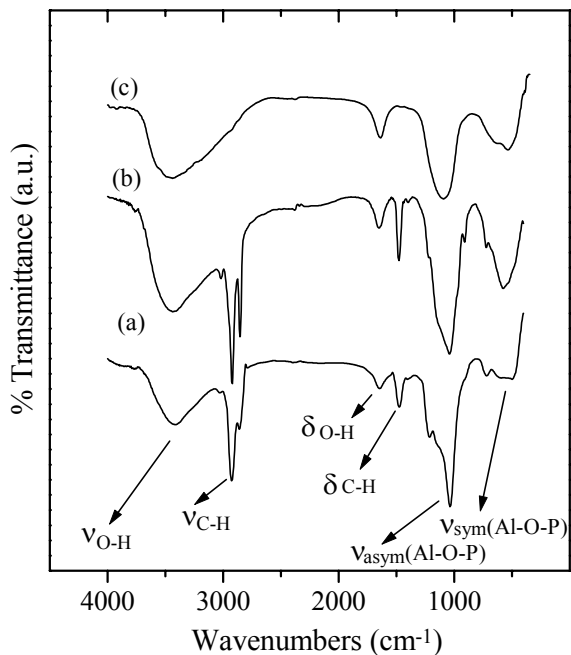


Figure 5. FT-IR spectra of: (a) as-synthesized LMA, (b) as-synthesized and (c) calcined HMA.

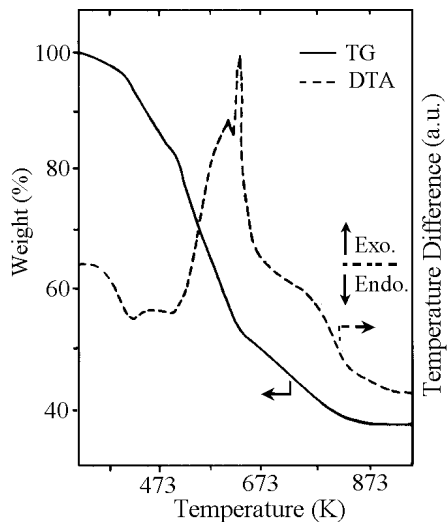


Figure 6. TG-DTA of as-synthesized HMA.

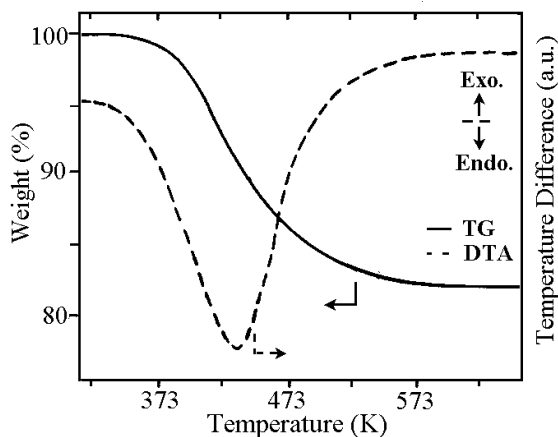


Figure 7. TG-DTA of calcined HMA.

N₂ sorption isotherms: Nitrogen adsorption-desorption (sorption) isotherm of calcined HMA showed type IV curve (Figure 8) typical for mesoporous molecular sieves.^{27,49} As the relative pressure increases ($P/P_0 > 0.2$), the isotherm exhibits an inflection characteristic of capillary condensation within the mesopores. Adsorption at low relative pressures ($P/P_0 < 0.2$) is caused by monolayer adsorption of N_2 on the walls of the mesopores.^{27,49} At $P/P_0 = 0.5$ the pore volume was calculated as $0.47 \text{ cm}^3 \text{ g}^{-1}$ with specific surface area, $985 \text{ m}^2 \text{ g}^{-1}$. A narrow pore size distribution was observed (Figure 8, inset) with mesopore diameter of 25 \AA . These values are in close agreement with the reported values for mesoporous aluminophosphates.

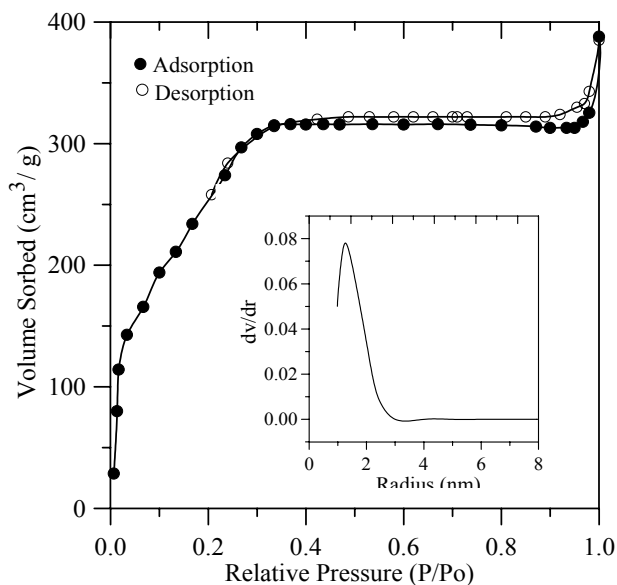


Figure 8. N₂ sorption isotherms of HMA (inset shows the pore size distribution).

MAS-NMR: MAS-NMR spectra confirms that the inorganic network consists of Al-O-P linkages. The ²⁷Al NMR spectra of as-synthesized HMA and calcined HMA are shown in Figure 9. All the spectra exhibit two main resonance, at ca 42 and 8 ppm, corresponding to tetrahedral Al(OP)₄ and octahedral Al(OP)₄(H₂O)₂, respectively.¹⁸ In the calcined sample, a slightly higher relative intensity of the octahedral resonance is observed than in the as-synthesized material, which can be explained by additional water ligands coordinating to Al after the removal of templates. This observation of octahedral resonance is a common phenomenon in mesoporous aluminophosphates and is reported in almost all literatures reported so far. Thus in case of HMA, the inorganic network consists not only of tetrahedral aluminium but also tricoordinated aluminium or aluminum oxide or oxyhydroxide species (with octahedral Al, presumably γ -AlO(OH), boehmite).^{17,50,51} This observation is supported by ICP-AES analysis where Al/P ratio was observed more than one. Figure 10 shows the ³¹P MAS-NMR spectra of as-synthesized and calcined HMA samples. The occurrence of ³¹P chemical shift as -14 ppm is due to tetrahedral phosphorous bonded to four aluminium ions via oxygen bridges, as a P(OAl)₄ unit, whereas the lines in 0 to -5 ppm range are assigned to phosphorous atoms with mixed

coordination P(OH)_x(OAl)_{4-x}, where x is 1-3.²⁷ This interpretation supports that there is no strict aluminium and phosphorous ordering of alternating AlO₄ and PO₄ structural units in these aluminophosphate-based mesoporous molecular sieves. The other peaks (marked by asterisks) are spinning sidebands. The spectrum of AlPO₄ is also shown in Figure 10.

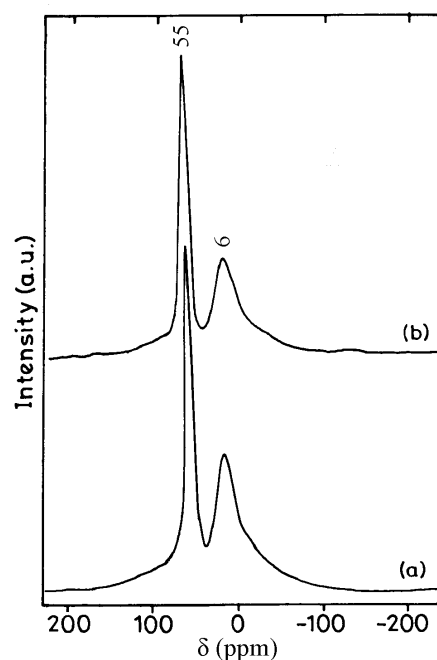


Figure 9. ²⁷Al MAS-NMR of: (a) as-synthesized HMA and (b) calcined HMA.

NH₃-TPD: Figure 11 displays the NH₃-TPD (TPDA) profile of HMA. The desorption pattern consists of two distinct peaks concentrated at 438 K and 845 K. The desorption peak at lower temperature range mostly consists of P-OH or Al-OH defect sites in the matrix.⁵⁰⁻⁵² The broadness of this peak, which gives rise to two peaks after deconvolution indicates two types of Brønsted acid sites (weak and moderate) that are present in the matrix. In microporous aluminophosphates, it has been shown that by the partial hydrolysis of Al-O-P bonds according to the reaction: -Al-O-P- + H₂O \leftrightarrow -Al-OH + HO-P-, weak Brønsted acid sites arise.⁵³ We expect the same phenomenon is occurring for mesoporous aluminophosphates also. On the other hand, the peak at higher temperature range may form due to the presence of tricoordinated aluminium or octahedral aluminium oxide or

oxyhydroxide species present in the matrix due to incomplete condensation of Al-O-P network,^{50,51,54} which is in accordance with the results obtained from MAS-NMR and ICP-AES studies. The generation of Brønsted and Lewis acidity in HMA is shown in Scheme 1.

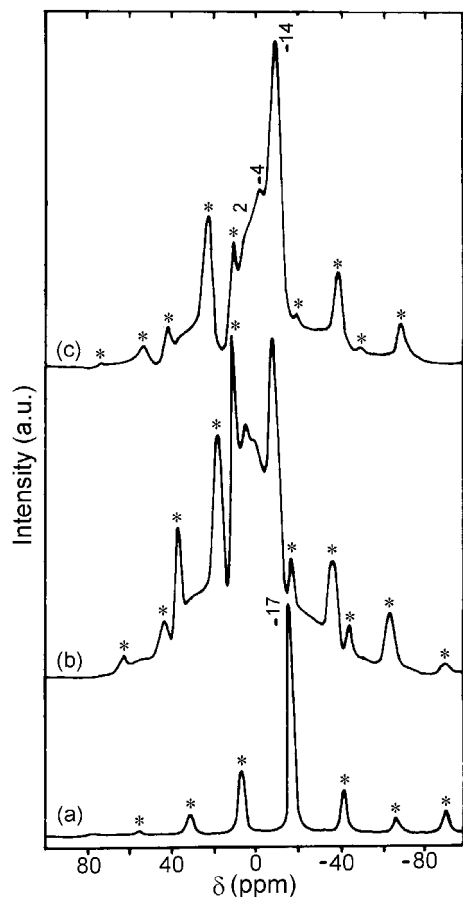


Figure 10. ³¹P MAS-NMR of: (a) AlPO₄, (b) as-synthesized HMA and (c) calcined HMA. Asterisks denote spinning side bands.

Formation mechanism of HMA

All these studies indicate that the amount of TMAOH plays a vital role in the formation of HMA. When the TMAOH was replaced by NaOH / KOH and pH was adjusted to 10, mesostructured material was not obtained. Thus TMA ion has a major role in the formation mechanism of the phases. However, in general, the mechanism of the formation of mesostructure aluminophosphates is not well studied due to the complexity in the transformation of the two HMA and LMA phases. Kuroda et. al.²⁵ proposed the formation of HMA from LMA under stirring in water.

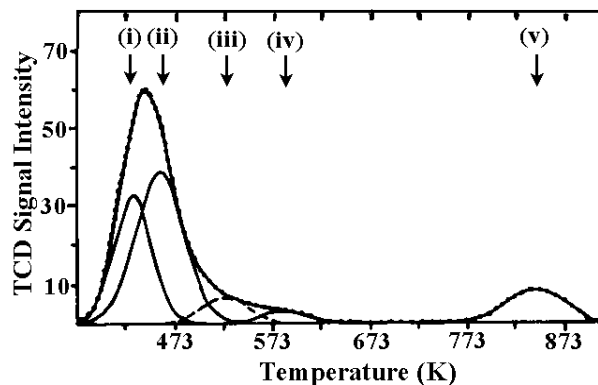
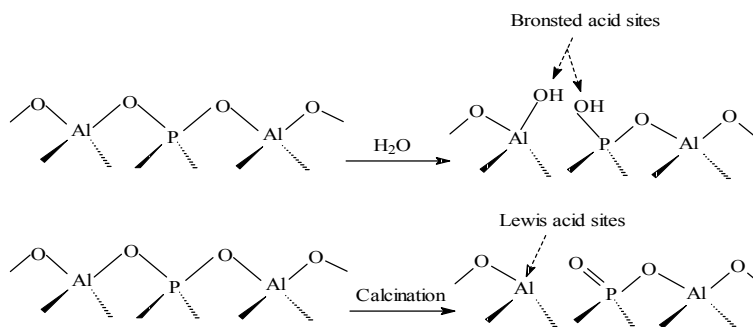


Figure 11. NH₃-TPD of calcined HMA.



Scheme 1. Brønsted and Lewis acid sites in HMA.

Kevan et. al.²⁷ generalized the formation of HMA as the self assembly process involving electrostatic interactions between positively charged quaternary ammonium surfactants (S⁺) and inorganic ions (Γ) in the presence of the organic base TMAOH. The inorganic precursors (Γ) are aluminophosphate species of low polymerization degree with some hydroxyl groups. When an organic base TMAOH is added, the tetramethylammonium ion TMA⁺ reacts with the hydroxyl group of these aluminophosphate species to produce a relatively weak ion pair (I⁻...TMA⁺) since the TMA ion has a large ionic radius. These ion pair species diffuse to the surfactant assembly interface and interact with the cationic surfactant headgroups. The interaction of the negatively charged aluminophosphate species with the cationic surfactant headgroups is stronger than with the TMA⁺ cation. Thus in a similar way to mesoporous silicates,⁵⁵ the micelles organize either in the form of disordered (tubular) / ordered hexagonal or lamellar structure depending on the synthesis condition, followed

by the polymerization of the aluminophosphate species (Figure 12). It is, however, to be noted here that upon calcination the ordered HMA (*see* Figure 2a) transform into disordered HMA (*see* Figure 2b). On the other hand, upon calcination, the disordered hexagonal or tubular structure transform into highly disordered or amorphous materials.

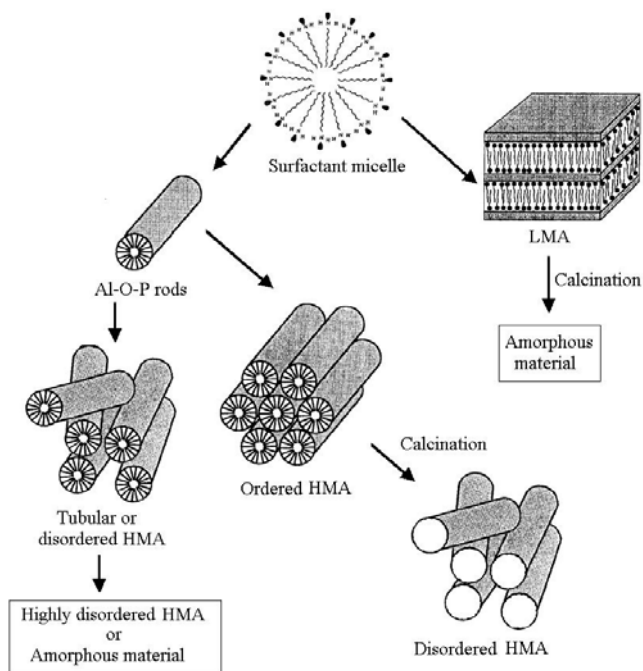


Figure 12. Schematic representation of the formation of LMA and HMA structures.

The function of the organic ammonium cation from TMAOH is to modify the strength of the electrostatic interaction between the aluminophosphate species and the cationic surfactant micelle assembly to form a $S^{+}I^{-}TMA^{+}$ ion pair. If NaOH / KOH are used, the Na^{+} cation with a smaller ionic radius than TMA^{+} has a stronger ion pair interaction with the aluminophosphate species and prevents sufficient interaction with the cationic surfactant assembly. Thus only amorphous material forms with inorganic bases. However, some more detailed studies need to be done to draw a firm conclusion.

CONCLUSION

In this investigation, both hexagonal and lamellar mesostructured aluminophosphate molecular sieves were synthesized using cationic

surfactant (CTAC) in presence of TMAOH. Upon calcination, the former, i.e., hexagonal mesostructured aluminophosphate (HMA) retains the mesoporous structure while the latter, viz., lamellar mesostructured aluminophosphate (LMA) phase collapses. Further, it was also deduced from this study that the hexagonal phase could be synthesized in very narrow range of gel composition and synthesis conditions. Although these materials have a tendency to transform into lamellar phase at higher temperature and longer duration of synthesis, the control of pH is a vital parameter to obtain thermally stable pure hexagonal phase.

ACKNOWLEDGEMENT

The authors thank SAIF/RSIC, IIT-Bombay for TEM, ED, TG-DTA, MAS-NMR and ICP-AES measurements.

REFERENCES

1. S.T. Wilson, B.M. Lok, C.A. Messina, T.R. Cannan and E.M. Flanigen, *J. Am. Chem. Soc.*, **104**, 1146 (1982).
2. M. Hartmann, and L. Kevan, *Chem. Rev.*, **99**, 635 (1999).
3. M. Estermann, L.B. McCuster, C. Baerlocher, A. Merrouche and H. Kessler, *Nature*, **352**, 320 (1991).
4. M.E. Davis, C. Saldarriaga, C. Montes, J. Graces and C. Crowder, *Nature*, **331**, 698 (1998).
5. C.T. Kresge, M.E. Leonowicz, W.J. Roth, J.C. Vartuli and J.S. Beck, *Nature*, **359**, 710 (1992).
6. D. Trong On, D. Desplandier-Giscard, C. Danumah and S. Kaliaguine, *Appl. Catal. A*, **222**, 299 (2001).
7. B. Kraushaar-Czarnetzka, W.H.J. Stork and R.J. Dogterom, *Inorg. Chem.*, **32**, 5029 (1993).
8. S.R.J. Oliver, A. Kuperman, A. Lough and G.A. Ozin, *Chem. Commun.*, 1761 (1996).
9. S.R.J. Oliver, A. Lough and G.A. Ozin, *Inorg. Chem.*, **37**, 5021 (1998).
10. S.R.J. Oliver and G.A. Ozin, *J. Mater. Chem.*, **8**, 1081 (1998).
11. A. Chenite, Y.L. Page, V.R. Karra and A. Sayari, *Chem. Commun.*, 413 (1996).
12. A. Sayari, V.R. Karra, J.S. Reddy and I.L. Moudrakovski, *Chem. Commun.*, 411 (1996).
13. A. Sayari, I.L. Moudrakovski, J.S. Reddy, C.I. Ratcliffe, J.A. Ripmeester and K.F. Preston, *Chem. Mater.*, **8**, 2080 (1996).

14. Q. Gao, R. Xu, J. Chen, R. Li, S. Li, S. Qiu and Y. Yue, *J. Chem. Soc., Dalton Trans.*, 3303 (1996).
15. Q. Gao, J. Chen, R. Xu and Y. Yue, *Chem. Mater.*, 9, 457 (1997).
16. S. Cheng, J. Tzeng, and B. Hsu, *Chem. Mater.*, 9, 1788 (1997).
17. M. Froba and M. Tiemann, *Chem. Mater.*, 10, 3475 (1998); *Chem. Mater.*, 13, 3217 (2001); *Chem. Commun.*, 406 (2002).
18. M. Schultz, M. Tiemann, M. Froba and C. Jager, *J. Phys. Chem. B*, 104, 10473 (2000).
19. M. Tiemann, M. Froba, G. Rapp and S. Funari, *Chem. Mater.*, 13, 1342 (2000).
20. Y.J. Khimiyak and J. Klinowski, *J. Chem. Soc., Faraday Trans.*, 94, 2241 (1998); *Chem. Mater.*, 10, 2258 (1998).
21. P. Feng, Y. Xia, J. Feng, X. Bu and G.D. Stucky, *Chem. Commun.*, 949 (1997).
22. P. Feng, J. Feng, X. Bu and G.D. Stucky, *Inorg. Chem.*, 39, 2 (2000).
23. J. Perez, R.B. Borade and A. Clearfield, *J. Mol. Str.*, 469, 221 (1998).
24. Z. Yuan, T. Chen, J. Wang and H. Li, *Coll. Surf. A*, 179, 253 (2001).
25. T. Kimura, Y. Sugahara and K. Kuroda, *Chem. Lett.*, 983 (1997); *Chem. Commun.*, 559 (1998); *Micropor. Mesopor. Mater.*, 22, 115 (1998); *Chem. Mater.*, 11, 508 (1999).
26. D. Zhao, Z. Luan and L. Kevan, *Chem. Commun.*, 1009 (1997); *J. Phys. Chem.*, 101, 6943 (1997).
27. Z. Luan, D. Zhao, H. He, J. Klinowski and L. Kevan, *J. Phys. Chem.*, 102, 1250 (1998).
28. Z. Luan, D. Zhao, H. He and L. Kevan, *Micropor. Mesopor. Mater.*, 20, 93 (1998).
29. B.T. Holland, P.K. Isbester, C.F. Blanford, E.J. Munson and A. Stein, *J. Am. Chem. Soc.*, 119, 6796 (1997).
30. B.T. Holland, P.K. Isbester, E.J. Munson and A. Stein, *Mater. Res. Bull.*, 34, 471 (1999).
31. D.A. Kron, B.T. Holland, R. Wipson, C. Maleke and A. Stein, *Langmuir*, 15, 8300 (1999).
32. B. Chakraborty, A.C. Pulikottil, S. Das and B. Viswanathan, *Chem. Commun.*, 911 (1997); *Appl. Catal. A*, 167, 173 (1998).
33. C. Subrahmanyam, B. Louis, R. Fabio, B. Viswanathan, A. Renken and T.K. Varadarajan, *Catal. Commun.*, 3, 45 (2002).
34. C. Subrahmanyam, B. Louis, F. Rainone, R. Fabio, B. Viswanathan, A. Renken and T.K. Varadarajan, *Appl. Catal. A*, 241, 205 (2003).
35. S. Cabrera, J.E. Haskouri, C. Guillem, A. Beltran-Porter, D. Beltran-Porter, S. Mendioroz, M.D. Marcos and P. Amoros, *Chem. Commun.*, 333 (1999).
36. Y.Z. Khimiyak and J. Klinowski, *Phys. Chem. Chem. Phys.*, 2, 5275 (2001); *Phys. Chem. Chem. Phys.*, 3, 1544 (2001); *J. Mater. Chem.*, 12, 1079 (2002).
37. M.P. Kapoor and A. Raj, *Appl. Catal. A*, 203, 311 (2000).
38. X.S. Zhao and G.Q. Lu, *Micropor. Mesopor. Mater.*, 44-45, 185 (2001).
39. X.S. Zhao, G.Q. Lu, A.K. Whittaker, J. Drennan and H. Xu, *Micropor. Mesopor. Mater.*, 55, 51 (2002).
40. N.C. Masson and H.O. Pastore, *Micropor. Mesopor. Mater.*, 44, 173 (2001).
41. S.K. Mohapatra, B. Sahoo, W. Keune and P. Selvam, *Chem. Commun.*, 1466 (2002).
42. S.K. Mohapatra and P. Selvam, *Top. Catal.*, 22, 17 (2003).
43. S. K. Mohapatra, F. Hussain and P. Selvam, *Catal. Commun.*, 4, 57 (2003).
44. S. K. Mohapatra, F. Hussain and P. Selvam, *Catal. Lett.*, 85, 217 (2003).
45. P.T. Tanev and T.J. Pinnavaia, *Science*, 267, 865 (1995).
46. S.A. Bagshaw, E. Prouzet and T.J. Pinnavaia, *Science*, 269, 1242 (1995).
47. R. Ryoo, J.M. Kim and C.H. Ko, *J. Phys. Chem.*, 100, 17718 (1996).
48. R. Szostak, *Molecular Sieves, Principles of Synthesis and Identification*, Van Nostrand Reinhold, New York, pp.253, (1989).
49. S. Storck, H. Bretinger and W.F. Maier, *Appl. Catal. A*, 174, 137 (1998).
50. D. Arias, I. Campos, D. Escalante, J. Goldwasser, C.M. Lopez, F.J. Machado, B. Mendez, D. Moronta, M. Pinto, V. Sazo and M.M.R. de Agudelo, *J. Mol. Catal. A*, 122, 175 (1997).
51. E. Dumitriu, V. Hulea, I. Fechet, A. Auroux, J-F. Lacaze and C. Guimon, *Micropor. Mesopor. Mater.*, 43, 341 (2001).
52. J. Das, C.V.V. Satyanaryana, D.K. Chakraborty, S.N. Piramanayagam and S.N. Shringi, *J. Chem. Soc., Faraday Trans.*, 88, 3255 (1992).
53. B. Parlitz, U. Lohse and E. Schreier, *Micropor. Mater.*, 2, 223 (1994).
54. H. Kosslick, G. Lischke, H. Landmesser, B. Parlitz, W. Storek and R. Fricke, *J. Catal.*, 176, 102 (1998).
55. P. Selvam, S.K. Bhatia and C. Sonwane, *Ind. Eng. Chem. Res.*, 40, 3237 (2001).